

INTERNATIONAL JOURNAL OF ELECTRONICS AND COMMUNICATION ENGINEERING & TECHNOLOGY (IJECEET)

ISSN 0976 – 6464(Print)

ISSN 0976 – 6472(Online)

Volume 5, Issue 12, December (2014), pp. 266-275

© IAEME: <http://www.iaeme.com/IJECEET.asp>

Journal Impact Factor (2014): 7.2836 (Calculated by GIS)

www.jifactor.com

IJECEET

© IAEME

ANALYSIS OF DIABETIC RETINOPATHY BY AUTOMATIC DETECTION OF EXUDATES

R S DESHMUKH

Department Electronics and Telecommunication, RCOE, Mumbai.-50

ABSTRACT

In this research paper, a method for automatic detection of Exudates in digital eye fundus image is described. To develop an automated diabetic retinopathy screening system, a detection of dark lesions in digital fundus photographs is needed. Exudates are the first clinical sign of diabetic retinopathy and they appear small white dots on retinal fundus images. The number of Exudates is used to indicate the severity of the disease. Early Exudates detection can help reduce the incidence of blindness. Here, a method for the automatic detection of Diabetic Retinopathy (ADDR) in color fundus images was analyzed. Different preprocessing, feature extraction and classification algorithms are used. The performance of the automated system is assessed based on Sensitivity and Specificity.

Keywords: Diabetic retinopathy, Exudates, optic disk and fundus image

1. INTRODUCTION

Eye is an organ associated with vision. It is housed in socket of bone called orbit and is protected from the external air by the eyelids. The cross section of the eye is as shown in Figure 1-1 while that of retina is as shown in Figure 1- 2

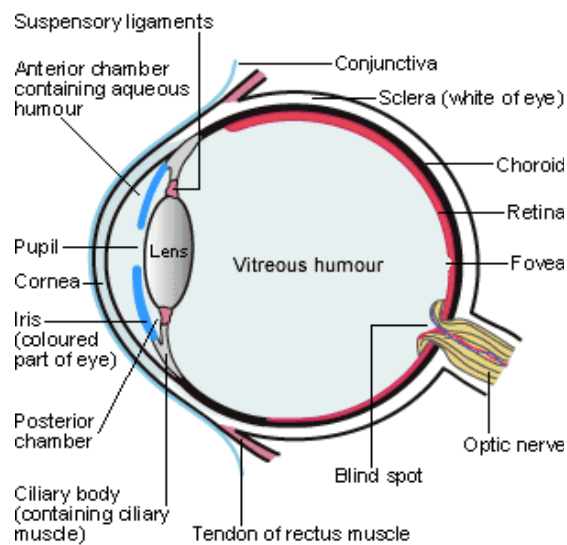


Fig 1-1. Structure of eye

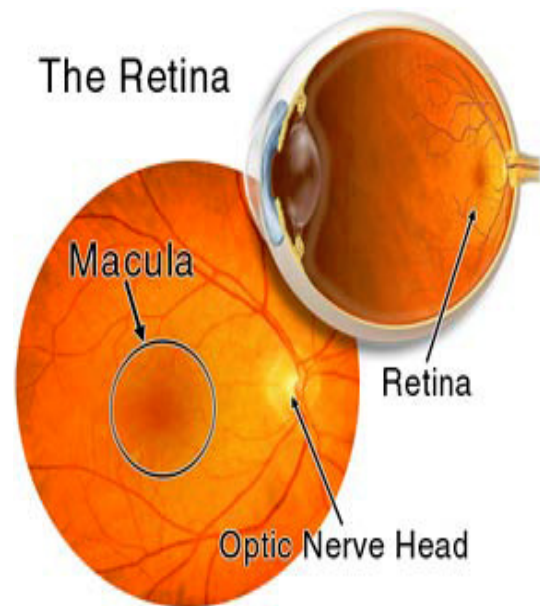


Figure 1-2. Retina Image

Light enters the eye through the pupil and is focused on the retina. The lens assists in focusing images from different distance. The amount of light entering the eye is controlled by the iris, by closing when light is bright and opens when light is dim. To the outside of the eye is a transparent white sheet called conjunctiva. Ciliary muscles in ciliary body control the focusing of lens automatically. Choroids form the vascular layer of the eye supplying nutrition to the eye structures. Image formed on the retina is transmitted to brain by optic nerve. Optic disk is brighter than any part of the retina image and is normally circular in shape. It is also the entry and exit point for nerves entering and leaving the retina to and from the brain. Near to the centre of the retina is an oval shape object called macula. The fovea is near the centre of the macula and it contains packed cone cells. Due to high amount of light sensitive cells, the fovea is responsible for the most accurate vision.

The retina is a multi-layered sensory tissue that lines the back of the eye. It contains millions of photoreceptors that capture light rays and convert them into electrical impulses. These impulses travel along the optic nerve to the brain where they are turned into images. There are two types of photoreceptors in the retina: rods and 8 cones. The retina contains approximately 6 million cones. The cones are contained in the macula, the portion of the retina responsible for central vision. They are most densely packed within the fovea, the very centre portion of the macula. Cones function best in bright light and allow us to appreciate colour.

Abnormalities Associated with the eye.

Abnormalities associated with the eye can be divided into two main classes, the first being disease of the eye, such as cataract, conjunctivitis, blepharitis and glaucoma. The second group is categorized as life style related disease such as hypertension, arteriosclerosis and diabetes. When the retina is been affected as a result of diabetes, this type of disease is called Diabetic Retinopathy (DR), if not properly treated it might eventually lead to loss of vision. Ophthalmologists have come to agree that early detection and treatment is the best treatment for this disease. DR occurrence have been generally categories into three main form viz, BDR, PDR, SDR. These Three classes can occur in any of the form described below as related to this research work ^[1-5].

Micro aneurysms: These are the first clinical abnormality to be noticed in the eye. They may appear in isolation or in clusters as tiny, dark red spots or looking like tiny haemorrhages within the light sensitive retina. Their sizes ranges from 10-100 microns i.e. less than 1/12th the diameter of an average optics disc and are circular in shape, at this stage, the disease is not eye threatening.

Haemorrhages: Occurs in the deeper layers of the retina and are often called ‘blot’ haemorrhages because of their round shape.

Hard exudates: These are one of the main characteristics of diabetic retinopathy and can vary in size from tiny specks to large patches with clear edges. As well as blood, fluid that is rich in fat and protein is contained in the eye and this is what leaks out to form the exudates. These can impair vision by preventing light from reaching the retina.

Soft exudates: These are often called ‘cotton wool spots’ and are more often seen in advanced retinopathy.

Neovascularisation: This can be describe as abnormal growth of blood vessels in areas of the eye including the retina and is associated with vision loss. This occurs in response to ischemia, or diminished blood flow to ocular tissues. If these abnormal blood vessels grow around the pupil, glaucoma can result from the increasing pressure within the eye [7]. These new blood vessels have weaker walls and may break and bleed, or cause scar tissue to grow that can pull the retina away from the back of the eye. When the retina is pulled away it is called a retinal detachment and if left untreated, a retinal detachment can cause severe vision loss, including blindness. Leaking blood can cloud the vitreous (the clear, jelly-like substance that fills the eye) and block the light passing through the pupil to the retina, causing blurred and distorted images. In more advanced proliferate retinopathy; diabetic fibrous or scar tissue can form on the retina.

2 DESIGN METHODOLOGY AND ALGORITHM

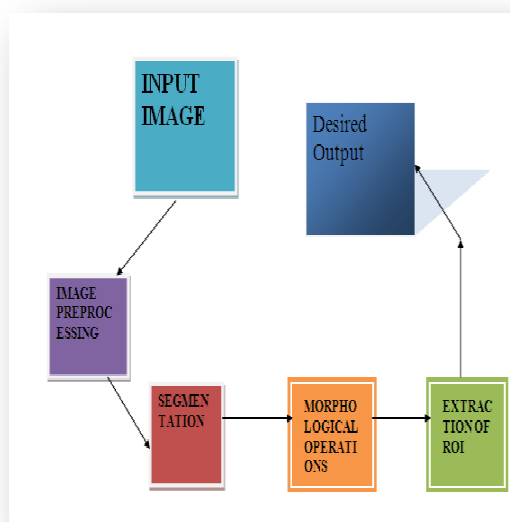


Fig 2. Matlab interface

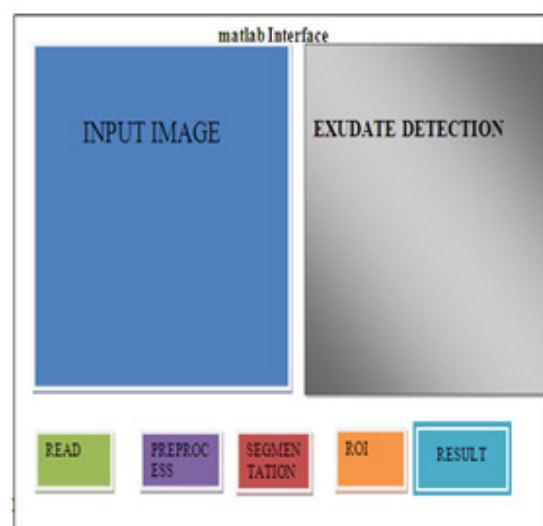


Fig 3. Morphological chart

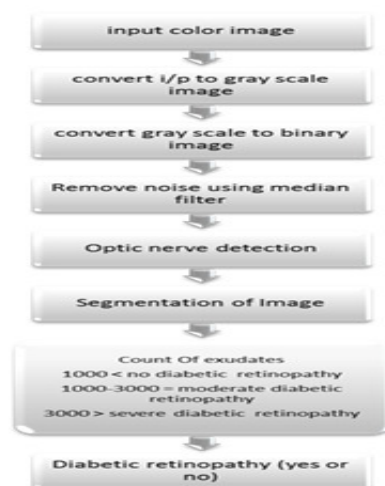


Fig 4. Block Diagram.

2.1 PRE PROCESSING

The aim of pre-processing is to attenuate the noise, to improve the contrast and to correct the non-uniform illumination. In the RGB images the green channel exhibits the best contrast between the vessels and background while the red and blue ones tend to be more noise. Hence green channel is used for further processing.

The next step is conversion of green channel image into a gray scale image, as the retinal blood vessels appear darker in the gray image. All the features like blood vessels, MAs etc are hidden in the background and are not clearly visible. Thus Normalization and contrast enhancement is performed to improve the image quality. Normalization is performed by subtracting an approximate background from the gray image. A 30x30 median filter is applied to the gray image and the result image is subtracted from green plane to get normalized image. Adaptive Histogram Equalization is applied for contrast enhancement. A dark region including vessels, MAs and noise are dominant after contrast enhancement⁶⁻¹⁰.

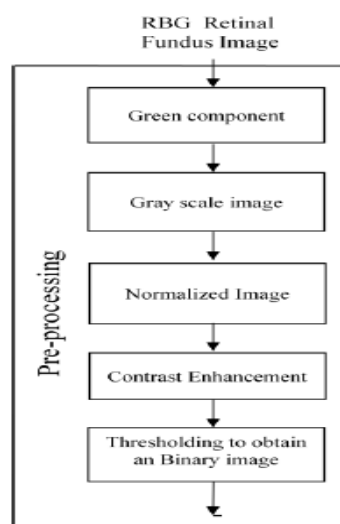


Fig 5. Preprocessing chart

The gray threshold is selected to determine the vessels and Exudates. The last step in the pre processing stage is binarization. The candidate vessels and MAs are then binarized by multi level thresholding. A correct threshold value is crucial, because smaller threshold value induces more

noise and higher threshold value causes loss of some fine vessels. Now the output image is ready for feature extraction.

2.2 Segmentation

As exudates are circular in shape, they can be identified from noise which is irregular in shape. Based on the major and minor axis, we can eliminate the noise having same area as exudates but is elongated in shape. Finally, exudates are detected based on perimeter and circularity. Canny edge detection is performed on the resulting image from the previous section. Each object's area and perimeter is calculated and these results are used to form a simple metric indicating the roundness of an object. The perimeter is calculated by finding the length of the boundary pixels of the candidate. In calculating perimeter, the x and y coordinates are counted as one and diagonal neighbors are counted $\sqrt{2}$ times¹¹⁻¹⁵.

Formulas for detection of circular objects

Delta = diff (boundary). ^2;

Perimeter = sum ((delta,))

Metric = $\frac{4\pi * \pi r^2}{(perimeter)^2}$

This metric is equal to one for a circle and it is less than one for any other shape. The discrimination process can be controlled by setting an appropriate threshold α .

$\alpha = \{0.94, 0.95, 0.96, 0.97, 0.98, 0.99, 1.00, 1.01, 1.02\}$

The similar formulas can also be used for the detection of optical nerve. For detection of optical nerve canny edge detection is applied only of optical nerve which is the maxima point in the fundus image. As the quality of fundus images is not too good for these images is the threshold value of for detection of optical disk is selected as 0.30 i.e. $\alpha = 0.30$ from trial and error method.

3. RESULTS AND DISCUSSIONS

For the purpose of evaluation 23 images were taken out of which 10 healthy, 7 moderate and 6 severe images were detected by designed algorithm.

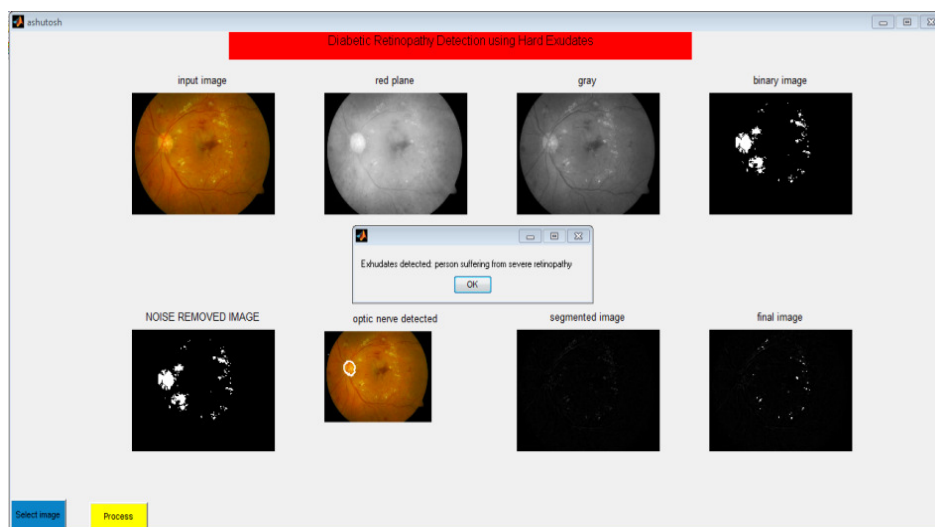


Fig 6. Result showing exudtaes.

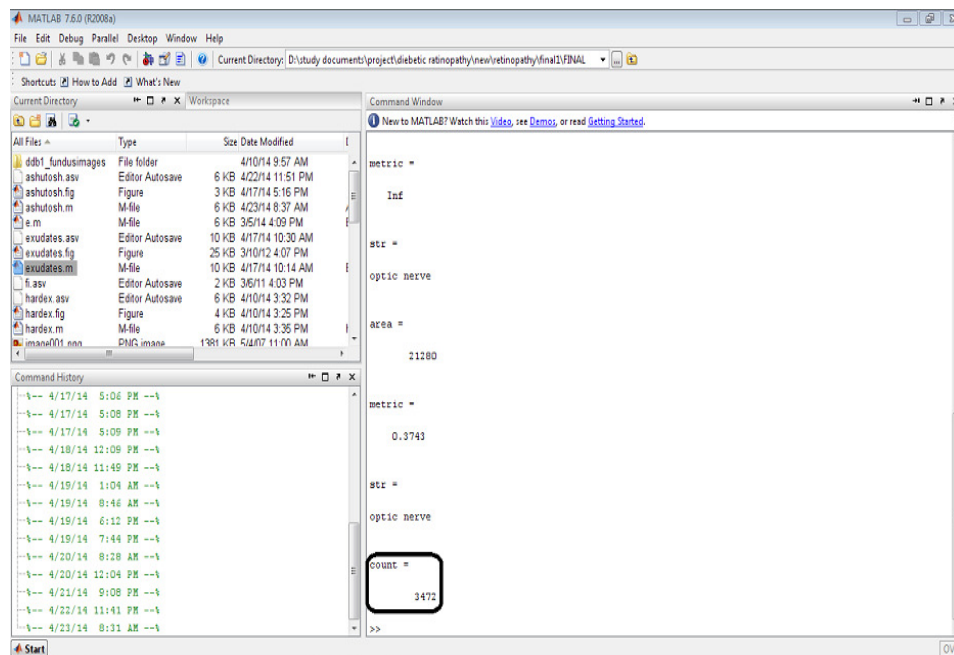


Fig 7. Pixels containing exudates

3. 1 Test Cases

Different grades of images with exudates detected by algorithm

In the testing of this project 23 fundus images were taken that are segmented in 3 different grades. The images in which pixel count is less than 1000 are healthy images, the counts between 1000 to 3000 are moderate risk and above 3000 are severe cases of retinopathy.

Table 1.Grading of fundus images

Grade	No. of Images	Range
(GRADE0)ABSENT	10	EXUDATE<1000
(GRADE1)MODERATE	7	1000<EXUDATE<3000
(GRADE2)SEVERE	6	EXUDATE>3000

Calculation of sensitivity, specificity, accuracy and precision:

Sensitivity and Specificity are the important parameters used to measure the accuracy of algorithm. The accuracy can be calculated based on True Positive (TP), False Positive (FP), True Negative (TN), and False Negative (FN).

True Positive - Abnormal images are correctly identified as abnormal.

False Positive - Normal images are incorrectly identified as abnormal.

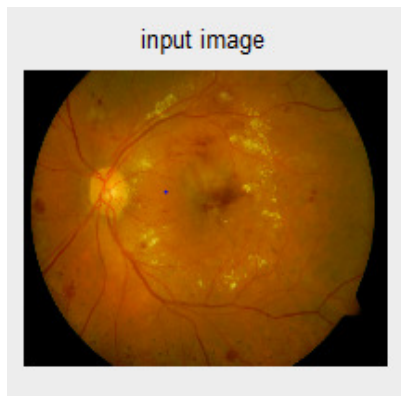
True Negative - Normal images are correctly identified as normal.

False Negative - Abnormal images are incorrectly identified as normal

Table 2. Tested result categories

TEST RESULT	PRESENT	ABSENT
POSITIVE	TRUE POSITIVE(TP)	FALSE POSITIVE(FP)
NEGATIVE	FALSE NEGATIVE(FN)	TRUE NEGATIVE(TN)

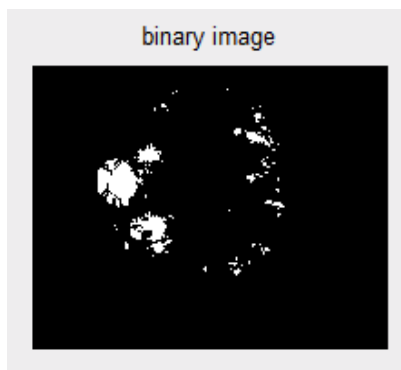
3.2 Segmentation of fundus image



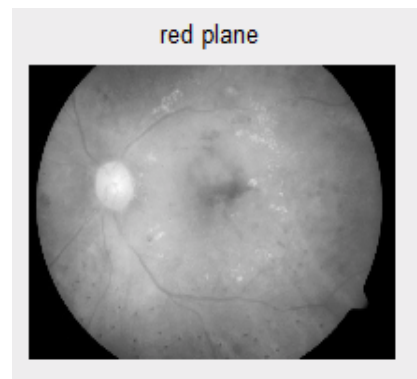
(a)



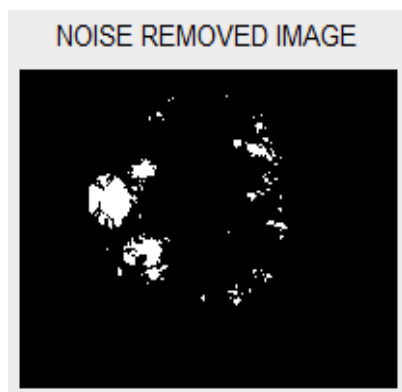
(b)



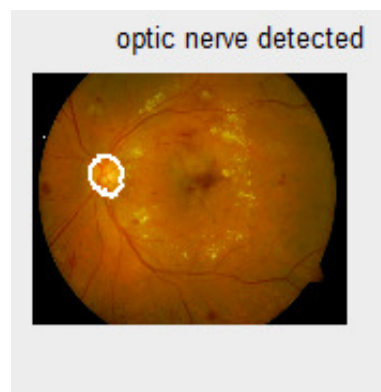
(c)



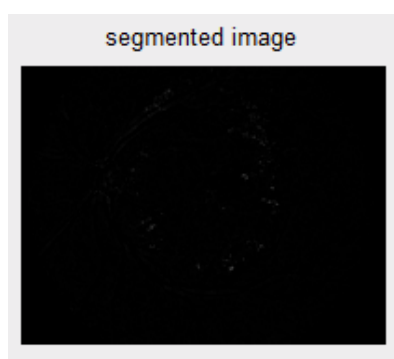
(d)



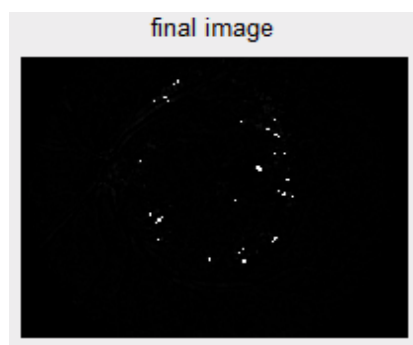
(e)



(f)



(g)



(h)

Results of evaluation fundus images

Table 3. Grading of images with number pixels contaminated with exudates

IMAGE	PIXELS CONTAINING EXUDATES	GRADE
IMAGE 1	3472(TP)	Severe
IMAGE 2	3577(TP)	Severe
IMAGE 3	5859(TP)	Severe
IMAGE 4	3910(TP)	Severe
IMAGE 5	125(TN)	No DR
IMAGE 6	61(TN)	No DR
IMAGE 7	2051(FP)	Moderate
IMAGE 8	34(FN)	No DR
IMAGE 9	709(FN)	No DR
IMAGE10	2277(TP)	Moderate
IMAGE 11	1(TN)	No DR
IMAGE 12	1(TN)	No DR
IMAGE 13	1881(TP)	Moderate
IMAGE 14	2277(TP)	Moderate
IMAGE 15	9(TN)	No DR
IMAGE 16	281(TN)	No DR
IMAGE 17	62(TN)	No DR
IMAGE 18	1(TN)	No DR
IMAGE 19	1259(TP)	Moderate
IMAGE 20	1080(TP)	Moderate
IMAGE 21	3597(TP)	Severe
IMAGE 22	3812(TP)	Severe
IMAGE 23	2389(TP)	Moderate

TP=12, TN=8, FP=1, FN=2

$$\text{SENSITIVITY} = \frac{TP}{TP+FN} = 86\%$$

$$\text{SPECIFICITY} = \frac{TN}{TN+FP} = 89\%$$

$$\text{ACCURAY} = \frac{TP+TN}{TP+FP+TN+FN} = 87\%$$

$$\text{PRECISION} = \frac{TP}{TP+FP} = 92\%$$

From Fig. 10 Sensitivity and the Specificity of various grades of images were calculated. The Sensitivity and Specificity for the designed algorithm is 86% and 89% respectively

Comparison of results obtained with other relevant research papers

From Table 4 and figure 8 the Sensitivity and Specificity of this project is compared with the other papers

Table 4. Comparison of results with other papers

Authors	Sensitivity	Specificity
Designed model	86%	89%
Giri Babu Kande	100%	87.5%
Abhir Bhalerao	82.6%	80.2%
Rumanao A	85.4%	83.1%

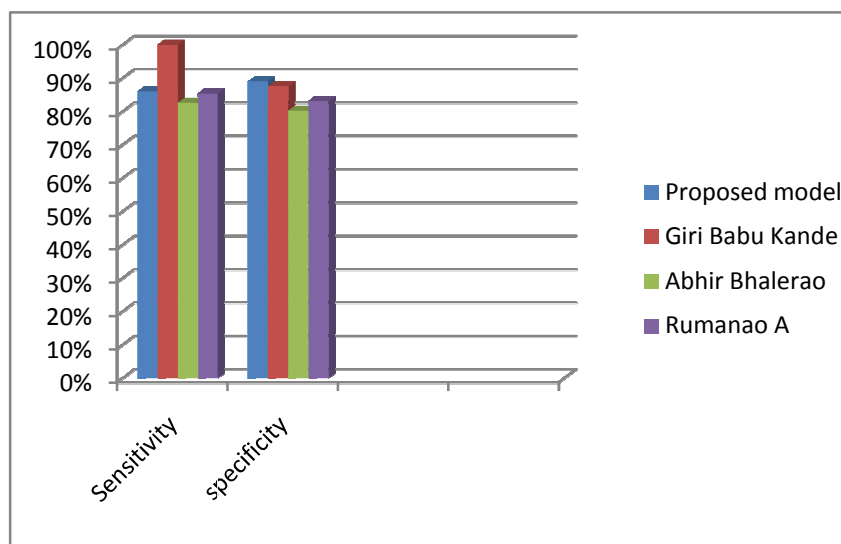


Fig 8: Sensitivity and Specificity comparison with other papers.

4. CONCLUSIONS

The outline of the research work concentrates on Hard Exudates detection in non- dilated digital images from diabetic retinopathy patients. The system intends to help the ophthalmologists in the diabetic retinopathy screening process to detect symptoms faster and more easily. The proposed algorithm could detect exudates on very poor quality images. The average sensitivity and specificity is 86% and 89% respectively. There are some incorrect exudates detections which are caused by the too small exudates, too blurred exudates, faint blood vessels which cannot be detected and removed. There are some missing exudates located next to or nearby blood vessels which are removed as wrongly detected as blood vessels. They are also faint blood vessels which are not removed in vessel detection step. Exudates could be wrongly detected on those vessels. Faint blood vessels can be incorrectly detected as exudates. A main weakness of the algorithm arises from the fact that the algorithm depends on white pixels which can be either exudates or noise particles. This indicates the further necessity of improving the robustness of this task. Micro aneurysms detection could be also added to the system in order to increase its ability to verify the degree of diabetic retinopathy.

REFERENCES

1. T. Spencer, J. A. Olson, K. C. McHardy, P. F. Sharp, and J. V. Forrester, "An image processing strategy for the segmentation and quantification of microaneurysms in fluorescein angiograms of the ocular fundus," *Computers and biomedical research*, vol. 29, no. 4, pp. 284–302, 1996.
2. T. Walter, J.-C. Klein, P. Massin, and A. Erginay, "A contribution of image processing to the diagnosis of diabetic retinopathy-detection of exudates in color fundus images of the human retina," *Medical Imaging, IEEE Transactions on*, vol. 21, no. 10, pp. 1236–1243, 2002.
3. M. Goldbaum, N. Katz, M. Nelson, and L. Haff, "The discrimination of similarly colored objects in computer images of the ocular fundus." *Investigative ophthalmology & visual science*, vol. 31, no. 4, pp. 617–623, 1990
4. D. S. Shin, N. B. Javornik, and J. W. Berger, "Computer-assisted, interactive fundus image processing for macular drusen quantitation," *Ophthalmology*, vol. 106, no. 6, pp. 1119–1125, 1999.
5. C. Sinthanayothin, J. F. Boyce, H. L. Cook, and T. H. Williamson, "Automated localization of the optic disc, fovea, and retinal blood vessels from digital colour fundus images," *British Journal of Ophthalmology*, vol. 83, no. 8, pp. 902–910, 1999.
6. D. Usher, M. Dumskyj, M. Himaga, T. Williamson, S. Nussey, and J. Boyce, "Automated detection of diabetic retinopathy in digital retinal images: a tool for diabetic retinopathy screening," *Diabetic Medicine*, vol. 21, no. 1, pp. 84–90, 2004.
7. M. Yulong and X. Dingru, "Recognizing the glaucoma from ocular fundus image by image analysts," in *Engineering in Medicine and Biology Society, 1990., Proceedings of the Twelfth Annual International Conference of the IEEE. IEEE, 1990*, pp. 178–179.
8. Z. Liu, C. Opas, and S. M. Krishnan, "Automatic image analysis of fundus photograph," in *Engineering in Medicine and Biology Society, 1997. Proceedings of the 19th Annual International Conference of the IEEE, vol. 2. IEEE, 1997*, pp. 524–525.
9. B. Kochner, D. Schuhmann, M. Michaelis, G. Mann, and K.-H. Englmeier, "Course tracking and contour extraction of retinal vessels from color fundus photographs: Most efficient use of steerable filters for model-based image analysis," in *Proceedings of the SPIE Conference on Medical Imaging*, vol. 3338, 1998, pp. 755–761.
10. K. Akita and H. Kuga, "A computer method of understanding ocular fundus images," *Pattern recognition*, vol. 15, no. 6, pp. 431–443, 1982.
11. T. Walter and J.-C. Klein, "Segmentation of color fundus images of the human retina: Detection of the optic disc and the vascular tree using morphological techniques," in *Medical Data Analysis. Springer, 2001*, pp. 282–287
12. F. Mendels, C. Heneghan, P. Harper, R. Reilly, and J.-P. Thiran, "Extraction of the optic disk boundary in digital fundus images," in *Proc. 1st Joint BMES/EMBS Conf, 1999*, p. 1139.
13. F. Zana and J.-C. Klein, "A multimodal registration algorithm of eye fundus images using vessels detection and hough transform," *Medical Imaging IEEE Transactions on*, vol. 18, no. 5, pp. 419–428, 1999
14. M. Niemeijer, "Retinopathy online challenge: Automatic detection of microaneurysms in digital color fundus photographs," *IEEE Trans. Med. Imaging*, vol. 29, p. 185–195, 2009.
15. L. Giancardo, F. Meriaudeau, T. P. Karnowski, Y. Li, S. Garg, K. W. Tobin, and E. Chaum, "Exudate-based diabetic macular edema detection in fundus images using publicly available datasets," *Med Image Anal*, vol. 16, no. 1, pp. 216–226, 2012..
16. R.S.Deshmukh, "Video Watermarking Schemes Based on Dwt and Pca Algorithm- A Novel Approach" *International Journal of Advanced Research in Engineering & Technology (IJARET)*, Volume 5, Issue 5, 2014, pp. 107 - 116, ISSN Print: 0976-6480, ISSN Online: 0976-6499.